JOURNAL OF AGRICULTURAL AND FOOD CHEMISTRY

New Device To Simulate Swallowing and in Vivo Aroma Release in the Throat from Liquid and Semiliquid Food Systems

KOEN G. C. WEEL,† ALEXANDRA E. M. BOELRIJK,*,† JACK J. BURGER,‡ MAYKEL VERSCHUEREN,† HARRY GRUPPEN,§ ALPHONS G. J. VORAGEN,§ AND GERRIT SMIT†,§

NIZO Food Research, Department of Flavor, Nutrition and Ingredients, P.O. Box 20, 6710 BA Ede, The Netherlands, Quest International Nederland BV, Naarden, The Netherlands, and Department of Agrotechnology and Food Sciences, Laboratory of Food Chemistry, Wageningen University, Wageningen, The Netherlands

This paper describes a novel device to simulate in vivo aroma release from liquids. This artificial throat simulates the act of swallowing followed by exhalation and shows aroma release curves that are similar in shape to in vivo release profiles. Liquids are poured down a tube, and a thin liquid film remains at the inner wall of the tube. Subsequently, aroma compounds release from this film into a stream of air flowing through this tube, which is analyzed by MS−Nose analysis. The effects of air flow rate, contact time with glass surface, presence of saliva, and addition of whey protein, as well as volume, concentration, temperature, and viscosity of the liquid have been studied and compared with aroma release measurements in vivo. A high level of agreement was found. These results confirm the importance of swallowing for aroma release of liquids, as mentioned in the literature, and the usefulness of the new mimicking device.

KEYWORDS: APCI-MS; MS−Nose; artificial throat; thin layer; viscosity; saliva

In recent decades, a lot of research has been dedicated to the development of model systems that should mimic the release of volatiles from food products during consumption. The advantages of having such devices are the possibility to save money and time spent on working with panelists, the omitting of palatability and safety matters, and a high reproducibility.

All model systems developed until now are designed to mimic the aroma release in the mouth and are based on the shared principle of a certain amount of foodstuff (usually in liquid form) containing aroma compounds and other ingredients of interest (polysaccharides, proteins, lipids) that is put into a vessel and stirred or shaken in different ways (and heated to 37 °C, in most cases) (*1*−*14*). Air is sampled from the headspace or nitrogen is purged through the liquid phase. The volatile compounds present in the stream of gas released from the model system are analyzed inline or batchwise by a direct mass spectrometry (MS) technique or by trapping the compounds on absorbing materials followed by gas chromatography−mass spectrometry (GC-MS) (*1*−*8*). All kinds of apparatus-related and product-related parameters have been studied using these model systems, which have increased insight in the process of volatile release in general (*9*−*14*).

For solid products, when structural breakdown in the mouth is involved, the aroma release can be reproducibly studied in Van Ruth's model mouth system (*2*) or the retronasal aroma simulator (RAS) (*3*). A computerized apparatus developed to simulate dynamic flavor release from liquids by Rabe and co-workers (*8*) focuses on simulation of events taking place in the mouth. The aroma release from liquid products, which are swallowed directly after intake, is determined by swallowing rather than by the preceding oral processing. This concept was first mentioned by De Roos and Wolfswinkel in 1994 (*15*) and again later, in 1996, when Land introduced the "swallow-breath" principle, which is 5−15 mL of air that is pushed through the nose immediately after swallowing and which had been in close masticatory contact with the food or drink in the mouth (*16*). This plug of air is important for aroma perception. Since the emergence of direct MS methods for sufficiently sensitive and fast real-time analysis of volatiles in human breath (*17*−*19*), it has become clear that the highest in vivo aroma release signal for liquids is generally found in the first exhalation after swallowing (*20*). It was shown that no gas is transferred from the oral cavity to the nasal cavity as long as no opening of the barrier formed by the tongue and the soft palate occurs by swallowing or by vigorous tongue and mouth movements (*21*). The existence of an anatomical barrier during the swallowing

* Corresponding author. Phone: +31318659638; fax: +31318659400; e-mail: Alexandra.boelrijk@nizo.nl.
† NIZO Food Research.
‡ Quest International Nederland BV.
§ Wageningen University.

10.1021/jf049499x CCC: $27.50
Published on Web 09/21/2004

process has been proven by videofluoroscopy and real-time magnetic resonance imaging (*22*). A protocol was developed in our laboratory that increased reproducibility of in vivo aroma release measurements of liquids by control of breathing and swallowing and thus reconfirming the importance of swallowing for release (*23*). In a recent study, Hogson and co-workers (*24*) combined synchronized measurements of mastication, swallowing, breath flow, and aroma release and demonstrated that an average chew displaces a volume of 26 mL of air from the oral cavity into the throat (which is especially relevant to the situation when the food is not swallowed immediately). Nasal airflow and associated aroma release were not detected during swallowing, but airflow and release were obvious directly after the swallowing event. The volume of the retronasal pathway was calculated to be 48 or 72 mL (depending on the type of calculation).

After swallowing, the majority of the sample disappears into the esophagus, but a thin layer of the liquid sample remains on the surface of the pharynx. Buettner and co-workers (*25*) visualized the formation of such a coating by videofluoroscopy, when a volunteer swallowed viscous oral contrast medium. A mathematical model was developed recently on the basis of this principle (*26*). During the exhalation following the swallowing, a steep gradient in aroma concentration exists between the thin liquid layer on the surface of the pharynx and the exhaled air that passes over this surface. It has been suggested that the major part of the aroma compounds present in this thin liquid layer coating the throat will release almost instantaneously during this exhalation because of the large surface area to volume ratio (*27*). A model system that aims to simulate the dynamic conditions of in vivo aroma release of liquids should therefore be able to simulate this process. Chewing-induced mixing and temperature changes of the sample during oral processing are only marginally important for aroma release from liquids because of the short residence time in the mouth and because the release is determined by the events taking place after swallowing. Thus, a model system is needed in which a thin layer of liquid is exposed to a relatively large flow rate to approach the dynamic in vivo release conditions. This paper describes the development, characterization, and comparison with in vivo release of such an artificial throat.

MATERIALS AND METHODS

Materials. Citral (mixture of geranial [67%] and neral [33%]) and geranyl acetate (ester of acetic acid and a mixture of 3,7-dimethyl-2-*trans*,6-octadien-1-ol [geranyl acetate, 67%] and 3,7-dimethyl-2-*cis*,6 octadien-1-ol [neryl acetate, 33%]) were obtained from Quest International B.V. (Naarden, The Netherlands). Butanal was obtained from Fluka Chemie (Buchs, Switzerland). Butane-2,3-dione, ethyl butanoate, hexanal, octanal, and nonanal were obtained from Merck (Darmstadt, Germany). κ-Carrageenan (extracted from Irish moss, batch 398961/1 40202) was obtained from Fluka Chemie (Buchs, Switzerland). Ethanol (>99.9%) was purchased from J. T. Baker (Deventer, The Netherlands). All solutions were prepared using demineralized water.

Whey protein isolate (Bipro, JE 153-9-420) was obtained from Davisco Foods International Inc., Le Sueur, MN. Specifications were as follows: pH 7.23; nonprotein nitrogen 0.17%; ash 1.8%; lactose 0.34%; calcium 0.13%; fat 0.57%; total protein 93.39% (N × 6.38); α-lactalbumin 12.6%; bovine serum albumin 3.2%; immunoglobulin G 5.2%; β-lactoglobulin A 33.2%; and β-lactoglobulin B 37.1%. A buffer was prepared with NaH_2PO_4. The pH was set with HCl.

Artificial saliva was prepared in demineralized water according to Van Ruth and co-workers (*2*) and consisted of $NaHCO_3$ (5.2 g/L), K_2HPO_4 (1.04 g/L), NaCl (0.88 g/L), KCl (0.24 g/L), $CaCl_2 \cdot 2H_2O$ (0.44 g/L), and 2.16 g/L porcine stomach mucin (Sigma, Steinheim, Germany). No α-amylase was added. The pH was set to 7.0 with HCl.

Table 1. Concentrations and Analysis Parameters of the Aroma Compounds

	concn in vivo (mg/L)	concn in AT[a] (mg/L)	ion mass (*m*/*z*)	cone voltage (V)
		Mixture 1		
butanal	2	0.1	73.0	21
hexanal	2	0.1	101.0	21
octanal	2	0.1	129.0	21
geranyl acetate	1	0.1	137.0	20
		Mixture 2		
butane-2,3-dione	25	1	86.6	19
ethyl butanoate	0.1	0.01	116.7	20
nonanal	2	0.1	143.0	21
citral	5	1	153.0	20

[a] Artificial throat.

Preparation of Solutions. Aroma solutions were prepared in two mixtures, one with a high concentration for in vivo measurements and another with low concentration for artificial throat, calibration, and static headspace measurements (**Table 1**). The use of a high and a low aroma concentration assured that the MS−Nose measurements had a high signal-to-noise level and linearity of response in all systems for each aroma compound. Ethanol was used to dissolve the compounds and was present at 0.01% (w/w) in all solutions used throughout the study. These aroma concentrations were used in aqueous solutions with either added whey protein or buffer, or carrageenan, or without any further additive, dependent on the experiment.

Whey protein solutions consisted of 50 mM NaH_2PO_4.HCl buffer (pH 7) with 3% (w/v) whey protein isolate. The aroma solutions without protein, to which the protein solutions were directly compared, also contained the same buffer. To dissolve the whey protein, the solutions were stirred for at least 3 h before addition of aroma.

Carrageenan solutions of 0.25, 0.50, and 0.75% (w/v) were heated at 70 °C for 30 min and first cooled to 50 °C before aroma was added. All solutions were stored in sealed containers at 4 °C until use.

Measurement of Aroma Release with the MS−Nose. Aroma concentrations in air coming from the artificial throat, the breath of panelists, static headspace flasks, or the glass vessel used for calibration were monitored by online sampling by an atmospheric pressure chemical ionization gas-phase analyzer (APCI-GPA) attached to a VG Quattro II mass spectrometer (MS−Nose; Micromass UK Ltd., Manchester, U.K.). The air was sampled (75 mL/min) through a capillary tube (0.53-mm internal diameter, heated to 100 °C). Source and probe temperatures were 80 °C. The compounds were ionized by a 3.0 kV discharge and monitored in selected ion mode (0.08 s dwell on each ion), in two independent sets. See **Table 1** for *m*/*z* values and cone voltages used. For in vivo experiments, acetone release was measured in both sets at 58.8 *m*/*z* (19 V) as an indicator of the panelists' breathing pattern. The chosen *m*/*z* values were unique for each compound. There was no difference in response between an aroma compound dissolved in a mixture and dissolved apart. None of the other ingredients used gave any signal at these masses.

Artificial Throat. In vivo aroma release was simulated by an artificial throat (**Figure 1**). This device consists of vertical glass tubing (internal diameter 12 mm). The MS−Nose sampling capillary samples air from the top end of the tube. An essential part of the system is a 3-mm-thick tubing of Viton rubber (11 mm i.d., DuPont Dow Elastomers L. L. C., Wilmington, DE) in the middle of the glass tubing that can be closed and opened by a clamp. Above this rubber section, several liquids can be added simultaneously or subsequently from syringes through capillaries, ending in the glass tubing. A water mantle surrounds the glass tubing and is coupled to a waterbath, equipped with a thermostat (set to 37 °C). An air inlet, which is pointing upward, is located below the water mantle. The liquid can leave the system from the down end of the glass tubing. This experimental setup is similar to falling film evaporators (*28*).

At the start of the experiment, the clamp is closed and 4 mL of liquid is loaded above the clamp. When using artificial saliva, 2 mL saliva is poured in first, followed by 2 mL aroma solution. After a

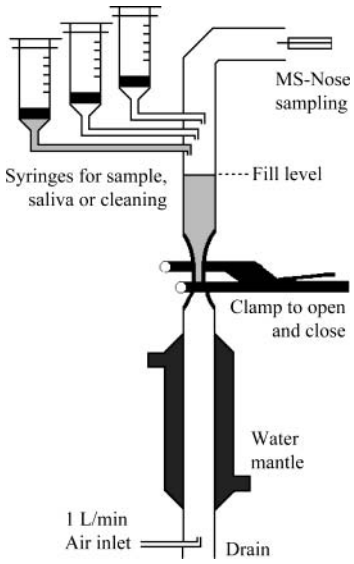

Figure 1. Schematic overview of the artificial throat configuration.

contact time of 10 s, the clamp is opened. The liquid pours down along the glass tubing. The wetted part is 30 cm (5 cm rubber and 25 cm glass). A thin liquid layer remains on the surface. Ten seconds after opening of the clamp, a stream of air (1.0 L/min) enters the tube and flows upward, where it can freely flow out of the system, while a small part of the air is sampled by the MS−Nose.

The inner glass surface was hydrophilized, by rinsing the surface with sulfuric acid (95−98% w/w). The glass kept its good wetting properties for over 50 measurements. The area below the release curve was integrated and used for calculation of the total amount of aroma released. Measurements were done in five replicates.

Measurement of in Vivo Aroma Release in Exhaled Air. Aroma release measurements in exhaled air were conducted using the MS−Nose according to a strict protocol, developed for liquid samples (*23*) to control chewing, breathing, and swallowing, to reduce experimental error. The area under the first exhalation peak after swallowing was integrated and used for calculation of the amount of aroma released in this breath. Two panelists were trained and considered to be sufficiently trained because their averaged relative standard deviation of the area for all samples of a training session did not exceed 15%. All samples were assessed in five replicates.

Static Headspace Measurements. Static headspace measurements were performed by inserting the sampling tip of the MS−Nose through a hole drilled in the cap of a 100-mL flask containing 20 mL of solution. Aliquots (10 mL) of human saliva (or water) and aroma solution were added and equilibrated for 10 min at ambient temperature before analysis in duplicate. This resulted in a plateau value from which an equilibrium aroma concentration in the sampled air could be calculated.

Calibration of Aroma Release Measurements. MS−Nose measurements were calibrated to quantify the results in vivo, in the artificial throat, and static headspace. An aliquot of 1 mL of aroma solution with a known concentration (concentrations used in artificial throat, **Table 1**) was put in a glass vessel (consisting of the mouth model described by Van Ruth and co-workers (*2*), without the plunger), which was connected to the MS−Nose sampling capillary. A magnetic stirrer mixed the liquid continuously. The headspace above this solution was continuously sampled into the MS−Nose source at a constant flow speed of 60 mL/min. The removed air was replaced by fresh air through a secondary opening. The release signal increased and subsequently returned to the baseline, indicating that all the aroma initially present in the solution had released. The area under this curve corresponds to the total amount of aroma present in the solution. Compounds were measured in two replicates. The concentration of the aroma compound in the air C_g (μg/L) can be calculated from the release signal in au (arbitrary units), according to eq 1.

$$C_g = \frac{M}{A \times F} \times \text{signal} \quad (1)$$

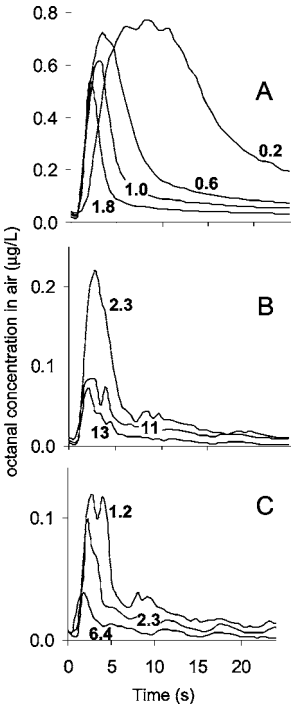

Figure 2. Release of octanal (0.1 mg/L in artificial throat, 2 mg/L in vivo) from an aqueous solution in either the artificial throat (**A**) or in vivo for panelists 1 and 2 (**B** and **C**, respectively), at different air flow rates (indicated in the graph in L/min; average relative standard deviation of 25%). Each curve is the average of five replicates.

in which M is the amount of aroma compound present in the solution (μg), A is the area under the calibration curve (au × min), and F is the flow of sampled air (L/min).

Breath Flow Measurement. Breath flow of panelists was measured using an ALNOR compuflow anemometer (Shoreview, MN), giving air speed in $m \cdot s^{-1}$, which was recalculated to a flow rate (L/min) using the diameter of the tube in the nose (5 mm).

Viscosity Measurements. Viscosity measurements were carried out with a Haake Rotovisco RV20 rotational viscometer (ThermoInstruments, Breda, The Netherlands). The concentric cylinder measuring system M5, equipped with the MV1 bob, was used. The radii of the bob and cup were 20.0 mm and 21.5 mm, respectively. The sample was subjected to a linearly increasing shear rate from 0 to 400 s^{-1} in 4 min and returning to 0 in 4 min, while the shear stress was measured. The dynamic viscosities quoted in this study were taken at a shear rate of 300 s^{-1}.

Measurement of Layer Thickness in Artificial Throat. The amount of liquid remaining in the artificial throat was determined by weighing the glass and rubber parts before (dry) and 10 s after pouring a sample through. The layer thickness could then be calculated in combination with the internal diameter and length of the tube.

RESULTS

Effect of Flow Rate. In **Figure 2**, typical examples are given of release curves obtained by the artificial throat and by in vivo release measurements. In the artificial throat, a solution containing 0.1 mg/L octanal was sampled at different air flow rates. Panelists were subjected to solutions of 2 mg/L octanal. The panelists breathed shallowly, normally, and deeply to obtain different flow rates. The flow rates differed considerably between panelists.

An increase in flow rate resu1ts in a decrease in the released peak area, both in vivo and in the artificial throat. This effect is observed for all aroma compounds studied. At a flow rate of 1.0 to 1.2 L/min, the peak width at 50% height in the artificial throat is typically around 5 s. This period is comparable to in

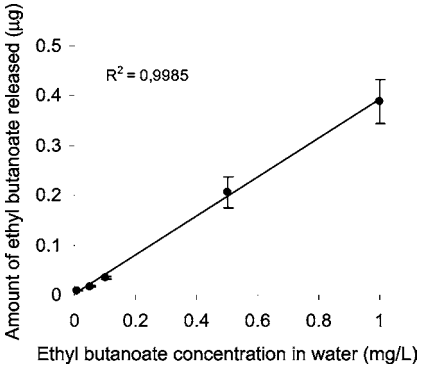

Figure 3. Released amounts of ethyl butanoate (μg) from the artificial throat at ethyl butanoate concentrations in the solution ranging from 0.01 to 1 mg/L. Error bars represent standard deviations.

vivo aroma release during shallow breathing (3 s in our in vivo protocol) and indicates the potential of the artificial throat to simulate the dynamics of in vivo aroma release of liquid foods. All further artificial throat measurements were performed at 1.0 L/min. This value fits into the flow rates measured in the present study for shallow breathing in vivo (1−2 L/min). The Reynolds number for air flow in the artificial throat was 134. A rough estimation of the Reynolds number in the human throat would be 1500. The Reynolds number for air flow in the human nose during exhalation has been reported to be 610 (*29*). Under the conditions used, the laminar flow is observed in the artificial throat as well as in vivo.

Effect of Sample Volume. The sample volume used in the artificial throat was varied between 2 and 4 mL. A different volume did not induce a significant difference in released peak area. The same result was found for in vivo measurements. A 4-fold increase of sample volume (from 5 to 20 mL) yielded only a less than 2-fold increase in in vivo released amount of aroma (data not shown). The amounts used differ between both systems for practical reasons, but the trends are the same.

Effect of Aroma Concentration. The aroma concentrations of the solutions show a high correlation with the released amount both in vivo and in the artificial throat. Linear relationships with high correlation coefficients were found for all compounds over an aroma concentration range of at least 2 orders of magnitude. An example of this, using the artificial throat, is given for ethyl butanoate in **Figure 3**.

Effect of Temperature. The temperature of the sample was varied from 5 to 66 °C, but this did not significantly change the release of any of the compounds studied either in vivo or in the artificial throat (data not shown).

Effect of Presence of Whey Protein. Previously, we have demonstrated that aldehyde retention in solutions containing whey protein isolate is less strong under in vivo conditions, compared to static headspace conditions (*27*). Here, the effect of presence of whey protein on release of aldehydes has been investigated in the artificial throat as well. The released amount of butanal, hexanal, octanal, and nonanal decreased because of the presence of 3% whey protein with 11%, 14%, 15%, and 20%, respectively.

Effect of Contact Time. The effect of differences in surface behavior between the human and the artificial throat can be visualized by changing the time between swallowing and exhalation in both systems. For the artificial throat, it is the time between opening of the clamp and application of the air flow. **Table 2** lists the relative change in released amounts of aroma for in vivo and artificial throat measurements because of longer delay time between swallowing and exhalation.

Table 2. Relative Change in Released Amounts of Aroma (Percent) from the Artificial Throat or in Vivo with 10 and 30 s between Swallowing and Exhalation, Compared to No Time In-Between

	artificial throat		panelist 1		panelist 2	
	10 s	30 s	10 s	30 s	10 s	30 s
butane-2,3-dione	–17	–25	–26	–45	–35	–64
ethyl butanoate	–17	–26	–38	–56	–20	–58
geranyl acetate	+3	–8	–46	–65	–41	–67
citral	–14	–24	–45	–70	–43	–73
butanal	–19	–15	–68	–78	–57	–77
hexanal	–25	–26	–66	–73	–54	–76
octanal	–15	–10	–70	–79	–66	–81
nonanal	–36	–43	–63	–78	–56	–88

Table 3. Persistence of Aroma Compounds in the Artificial Throat and Two Panelists[a]

compound	artificial throat	panelist 1	panelist 2
butane-2,3-dione	0.51 ± 0.017	0.74 ± 0.14	0.83 ± 0.11
ethyl butanoate	0.07 ± 0.0001	0.27 ± 0.0082	0.45 ± 0.041
geranyl ac	0.37 ± 0.060	0.54 ± 0.04	0.56 ± 0.068
citral	0.6 ± 0.066	0.52 ± 0.055	0.57 ± 0.052
butanal	0.07 ± 0.0063	0.21 ± 0.089	0.21 ± 0.10
hexanal	0.065 ± 0.0084	0.23 ± 0.085	0.18 ± 0.068
octanal	0.068 ± 0.0075	0.17 ± 0.043	0.16 ± 0.081
nonanal	0.072 ± 0.0084	0.23 ± 0.088	0.31 ± 0.097

[a] Persistence values in the artificial throat are calculated as the peak width at half-height in minutes. The in vivo persistence is calculated as the ratio between the peak height of the second and the first peak after swallowing. ± values indicate standard deviations.

Generally, the released amount of aroma drops as the contact time increases. This is observed in vivo with two panelists and in the artificial throat. However, the decrease is much stronger in vivo than with the artificial throat.

Persistence in the Breath. The in vivo persistence of the aroma compounds in the human breath can play a role in aftertaste. Persistence can be calculated according to the method of Linforth and Taylor (*20*). For the persistence in the artificial throat, the peak width at 50% of the peak height was taken. The results are displayed in **Table 3**. A high correlation between panelists was found for their persistence data ($R^2 = 0.91$) for the eight aroma compounds studied. The correlation between the artificial throat and the panelists was reasonable as well (R^2 was 0.70 and 0.82 for panelists 1 and 2, respectively).

Effect of Viscosity. The effect of viscosity on aroma release in vivo and in the artificial throat was studied by means of a range of aroma solutions with increasing carrageenan concentrations. The carrageenan solutions showed a lower dynamic viscosity at higher shear rates (shear-thinning behavior), but the curves of the increasing and decreasing shear rate closely overlapped, indicating that the solutions were not thixotropic. The results are shown in **Figure 4** for ethyl butanoate, butane-2,3-dione, and hexanal. An increase in viscosity results in an increase in released amount of aroma in the artificial throat. The other aroma compounds showed similar effects (results not shown).

The artificial throat measurements presented in **Figure 4** were conducted at a flow rate of 1.0 L/min. Measurements were also done using flow rates of 0.2, 0.6, 1.2, and 1.8 L/min (data not shown). Although the area under the release curve decreased with increasing flow rate (as shown in **Figure 2**), the qualitative effect of differences in viscosity was similar for each flow rate.

The measurements were repeated to investigate the influence of dilution with saliva on aroma release in the artificial throat.

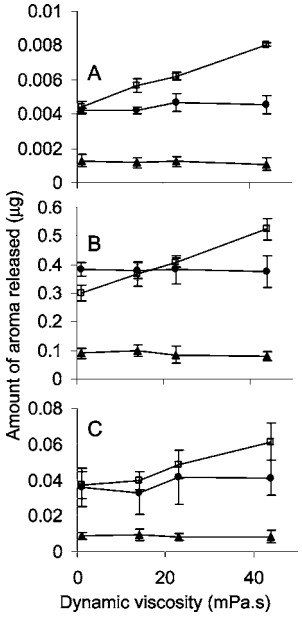

Figure 4. Released amounts (μg) of ethyl butanoate (**A**), butane-2,3-dione (**B**), and hexanal (**C**) with increasing dynamic viscosity (mPa.s) for the artificial throat (□), panelist 1 (●), and panelist 2 (▲). Error bars represent standard deviations.

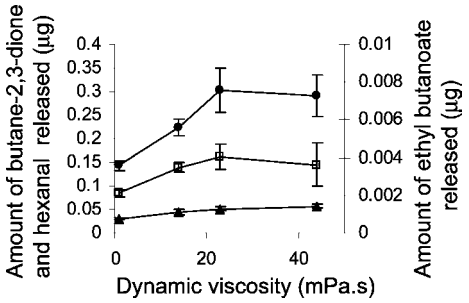

Figure 5. Released amounts (μg) of butane-2,3-dione (●), hexanal (▲), and ethyl butanoate (□) from 2 mL aroma solutions with increasing viscosity (mPa.s) in the artificial throat, with 2 mL artificial saliva added first. Error bars represent standard deviations. The viscosity on the *x*-axis reflects the viscosity in the aroma solution before mixing with water or saliva.

Now, 2 mL water or nonaromatized artificial saliva was added first, followed by 2 mL of an aroma solution with the same range of viscosities. Both solutions were poured into the artificial throat, without further external mixing. The results for ethyl butanoate, butane-2,3-dione, and hexanal with addition of artificial saliva are shown in **Figure 5**. The released amount of aroma increases going from low to high viscosities, reaching a plateau value at high viscosity. This was also observed for the other aroma compounds analyzed (results not shown). These results contrast to the effect of viscosity without addition of water or saliva, which displayed a steady increase within the viscosity range studied. No differences were found between the results obtained with addition of artificial saliva and those with water for all aroma compounds examined (no further results shown, ANOVA, $p = 0.18$).

DISCUSSION

Aroma Release from Thin Liquid Layer. The design of the artificial throat was inspired on the hypothesis that the majority of aroma release from liquids in vivo originates from the layer that remains at the inner surface of the human throat after swallowing (*27*). The results obtained here are well in line with this hypothesis. The effects of sample volume, aroma concentration, sample temperature, air flow rate, and presence of whey protein show similar trends in the artificial throat compared to in vivo, as will be discussed below.

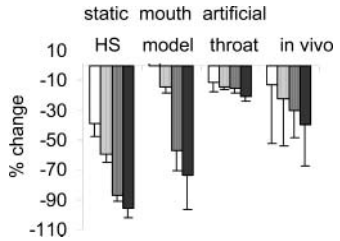

Figure 6. Relative change (%) in release of butanal (white bars), hexanal (light gray bars), octanal (dark gray bars), and nonanal (black bars) because of presence of 3% whey protein for different systems (graph contains data from Weel et al. (*27*)). Error bars represent standard deviations.

With respect to the sample volume, the released amount of aroma is only slightly dependent on the sample volume. The reason for this is probably that the liquid-layer thickness is only slightly dependent on the amount of liquid passing through as long as the total amount is much larger than the amount constituting the film at the inner surface. When the aroma concentration is higher (**Figure 3**), there is proportionally more aroma compound available for release. Linear increase in in vivo aroma release with liquids with increasing aroma concentrations was found previously as well (*23*).

The sample temperature does not influence the total aroma release, either in vivo or in the artificial throat, because all aroma present in the thin film will rapidly release, once the exhalation or air flow starts. At equilibrium conditions, however, a higher temperature leads to a stronger partitioning of volatiles into the air phase. This has been demonstrated previously for a range of aroma compounds (*3*, *30*).

A decrease in measured release with increasing flow rate is also expected (**Figure 2**), because only a part of the air exhaled either by the artificial throat or the panelists is sampled. The aroma concentration is determined in the part sampled. When the flow rate is higher, the aroma compounds are more diluted, resulting in a lower concentration. The total released amount of aroma does not change within the range of flow rates studied, because all aroma compounds present will release. The decrease in peak width at higher flow rate indicates that the reservoir of aroma molecules present in the thin liquid film (coating the inner surface of both the human throat and the artificial throat) is exhausted faster.

Aldehyde−protein interactions and their effect on aldehyde release have been investigated previously for static headspace, mouth model, and in vivo measurements (*27*, *31*, *32*). Considerable reversible interactions were found during static headspace measurements (binding up to 90%). These interactions appeared to be much less pronounced under in vivo conditions. Given a reversible interaction, it was hypothesized earlier (*27*) that after swallowing all aldehydes present in the layer coating the inner throat would release—the free aldehydes as well as those reversibly bound to the protein. This explanation is similar to the "thin-layer" hypothesis formulated above. **Figure 6** gives an indication of the interaction between a homologous range of aldehydes and whey protein in the artificial throat, the mouth model, under in vivo conditions, and static headspace (HS). From **Figure 6** it is clear that the results obtained in vivo and in the artificial throat deviate from the results obtained with static headspace and the mouth model. The interactions between

Table 4. Total Released Amount of Aroma during One Artificial Throat Run (Micrograms)[a]

compound	based on area integrated	based on film weight
butane-2,3-dione	0.36	0.33
ethyl butanoate	0.0054	0.0033
geranyl acetate	0.041	0.033
citral	0.32	0.33
butanal	0.039	0.033
hexanal	0.047	0.033
octanal	0.047	0.033
nonanal	0.041	0.033

[a] The amount is calculated on the basis of either the integrated release peak area or the weight of the film remaining on the glass wall.

aldehydes and protein under in vivo and artificial throat conditions are much less pronounced than under static headspace and mouth model conditions.

The assumption that all aroma present in the thin layer remaining in the human throat after swallowing will release was verified using the artificial throat. For this purpose, the total amount of aroma released during artificial throat measurements was calculated in two independent ways. The total amount of aroma released (and thus the amount of aroma initially present in the liquid film) could be calculated from the area integrated below the release curve. The other approach was to weigh the amount of liquid in the film at the glass wall and the rubber and to combine it with the known aroma concentration in the solution to calculate the amount of aroma. Results of both calculations are shown in **Table 4**.

The amounts calculated on the basis of the two methods are both in the same order of magnitude and are highly correlated ($R^2 = 0.99$). Confirming our hypothesis, the bulk of the aroma compounds present in the liquid film in the artificial throat has indeed released within 10 s into the air flowing along the liquid film. Similarly to these results, the aroma present in the liquid layer in the human throat after swallowing will probably release rapidly as well. On the basis of the weight of the liquid film and the dimensions of the artificial throat, the layer thickness of the film was calculated to be 0.1 mm for the rubber part and 0.015 mm for the glass part.

Contact with Throat Surface. Gravity-driven clearance of the liquid layer on the glass surface is the major factor responsible for the decrease in release in the artificial throat at longer time intervals between opening of the clamp and application of the air flow (**Table 2**). In vivo, there are additional processes involved, probably explaining the stronger loss of aroma compounds there. These are fluid excretion of the mucosa and partitioning of the aroma compounds into the mucus (*25*, *27*). It was shown previously that the extent of the interaction between aroma compounds and mucosa depends heavily on the contact time. When aldehyde solutions were rinsed in the mouth for 3 s and subsequently expectorated, 1% had released into the air and 7% of the aldehydes could not be retrieved and were probably lost to the inside coating of the mouth (*27*). Buettner et al. (*25*) reported a decrease of 30−40% upon 10-min rinsing of pyrazine solutions in the mouth. The measurements presented do not reveal the absolute amount lost because of interaction with the inner surface of the human throat during the normal residence time of the film in the throat. Nevertheless, these results clearly show that the inner surface of the human throat is not as inert as the glass surface of the artificial throat.

Persistence data of artificial throat and in vivo measurements correlated well, despite the different calculation methods (**Table 3**). Especially, butane-2,3-dione showed a high persistence in both systems. Because of its high hydrophilicity, this compound remains in the liquid layer forming a reservoir for continued release. Linforth and Taylor (*20*) have shown that hydrophobicity and vapor pressure are the main predictors for in vivo persistence. In our present study, a high persistence is also observed in the artificial throat for butane-2,3-dione, indicating that presence of mucus is no prerequisite for high persistence and thus stressing the importance of the liquid layer for persistence. Hydrophobicity cannot fully explain the observed persistences, as can be seen for instance for citral, which combines a low hydrophilicity with a high persistence.

Sample Viscosity and Dilution with Saliva. The effect of viscosity was studied with and without addition of saliva. When the viscosity of the samples increases, a thicker layer remains at the inner surface of the tube. This thicker layer will contain proportionally more aroma compounds, and consequently the total released amount will be higher (**Figure 4**). Determining the increase in weight of the artificial throat after pouring the samples through revealed that the amount of liquid remaining at the inner surface of the artificial throat 10 s after opening the clamp had increased 5-fold when comparing solutions with a viscosity of 1 and 44 mPa.s (0.25 and 1.21 g, respectively). The released amount of aroma, however, increased less than 5-fold (**Figure 4**). This can be explained as follows. The time scale of diffusion (τ) is given by eq 2

$$\tau = \frac{L_D^{\,2}}{D} \qquad (2)$$

where L_D is the layer thickness (m), and D is the diffusion coefficient ($m^2 \cdot s^{-1}$). The value of D is approximately $5 \cdot 10^{-10}$ $m^2 \cdot s^{-1}$ (ranging from $1 \cdot 10^{-10}$ to $1 \cdot 10^{-9}$ $m^2 \cdot s^{-1}$ for small molecules in water, derived from the Hayduk−Minhas correlation) (*33*). Considering aqueous solutions, the time scale of diffusion is 0.5 s for the liquid layer on the glass tube (0.015 mm) and 20 s for the liquid on the rubber part (0.1 mm). When the amount of liquid remaining at the inner surface of the artificial throat is 5 times higher, the layer is approximately 5 times thicker as well (the layer is very thin compared to the diameter of the tube). The time scale of diffusion is 12.5 and 500 s for the viscous liquid layers on the glass tube and on the rubber part, respectively. Consequently, a prolonged tailing release is obtained. However, the peak tailing is too small to be included in the peak integration process, leading to the differences observed.

In contrast to the artificial throat results, in vivo measurements showed no effect of viscosity on the amount of aroma released (**Figure 4**). This can be caused by differences in swallowing mechanism and by dilution with saliva. Swallowing in the artificial throat is driven by gravity, while in vivo the liquid is forced downward by pharyngeal peristalsis. It seems reasonable to assume that the film formed in vivo will therefore be different. Future versions of the artificial throat should take peristalsis effects into account.

Dilution with saliva could play a role as well. When saliva or water is added to the artificial throat, the increase in release with higher viscosity levels off. In the measurements corresponding to the results in **Figure 5**, the viscous solution is injected above an equal amount of water or saliva before the clamp is opened. This situation lasts for 10 s but no stirring or mixing is imposed. Therefore, in the more viscous solution, the mixing is limited, resulting in an inhomogeneous distribution of aroma throughout the sample. Improper mixing results in less aroma on the wall, after the sample was poured down.

Dilution always occurs under in vivo conditions, and this could also explain why there is no effect of viscosity in vivo. In vivo aroma release measurements have demonstrated before that viscosity does not influence aroma release (*34*).

No difference was found between addition of artificial saliva and water. On the basis of previous work, reversible interactions between aroma compounds and saliva could be expected in static headspace measurements (*27*, *31*, *32*), but as was shown for the effect of presence of whey protein (**Figure 6**), reversible interactions are of minor importance in the artificial throat. This suggests that the role of saliva is dilution, rather than aroma binding, under these dynamic conditions.

This paper has focused on the importance for aroma release of a liquid layer remaining in the throat after swallowing, and a model system to simulate the liquid layer was presented. Obviously, the artificial throat does not perfectly simulate the events in the human throat; it merely serves as a proof of principle. Aspects of the design to be amended in future versions include the possibility to have a tidal air flow simulating breathing patterns more closely, the coupling of the artificial throat to a chewing device, control of temperature and humidity of the air, and the choice of tube material. The work presented here has demonstrated that the surface properties of the materials used (rubber and glass) can strongly influence the release profile.

The effect of emulsion properties on release of esters from oil-in-water emulsions was studied using the artificial throat and compared to release under in vivo and static headspace conditions. This study serves as an example of an application of the artificial throat (*35*).

ACKNOWLEDGMENT

Peter Davidson (Quest R&D) is acknowledged for his original idea of the artificial throat.

LITERATURE CITED

(1) Lee, W. E. A suggested instrumental technique for studying dynamic flavor release from food products. *J. Food Sci.* **1986**, *51*, 249−250.

(2) Van Ruth, S. M.; Roozen, J. P.; Cozijnsen, J. L. Comparison of dynamic headspace mouth model systems for flavour release from rehydrated bell pepper cuttings. In *Trends in Flavour Research*; Maarse, H., van der Heij, D. G., Eds.; Elsevier Science: Amsterdam, The Netherlands, 1994; pp 59−64.

(3) Roberts, D. D.; Acree, T. E. Simulation of retronasal aroma using a modified headspace technique: investigating the effects of saliva, temperature, shearing, and oil on flavor release. *J. Agric. Food Chem.* **1995**, *43*, 3, 2179−2186.

(4) Nassl, K.; Kropf, F.; Klostermeyer, H. A method to mimic and to study the release of flavour compounds from chewed food. *Z. Lebensm.-Unters.-Forsch.* **1995**, *201*, 62−68.

(5) Elmore, J. S.; Langley, K. R. Novel vessel for the measurement of dynamic flavor release in real time from liquid foods. *J. Agric. Food Chem.* **1996**, *44*, 3560−3563.

(6) Bakker, J.; Boudaud, N.; Harrison, M. Dynamic release of diacetyl from liquid gelatin in the headspace. *J. Agric. Food Chem.* **1998**, *46*, 2714−2720.

(7) Springett, M. B.; Rozier, V.; Bakker, J. Use of fiber interface direct mass spectrometry for the determination of volatile flavor release from model food systems. *J. Agric. Food Chem.* **1999**, *47*, 1125−1131.

(8) Rabe, S.; Krings, U.; Banavara, D. S.; Berger, R. G. Computerized apparatus for measuring dynamic flavor release from liquid food matrices. *J. Agric. Food Chem.* **2002**, *50*, 6440−6447.

(9) Deibler, K. D.; Lavin, E. H.; Linforth, R. S. T.; Taylor, A. J.; Acree, T. E. Verification of a mouth simulator by in vivo measurements. *J. Agric. Food Chem.* **2001**, *49*, 1388−1393.

(10) Roberts, D. D.; Elmore, J. S.; Langley, K. R.; Bakker, J. Effect of sucrose, guar gum, and carboxymethylcellulose on the release of volatile flavour compounds under dynamic conditions. *J. Agric. Food Chem.* **1996**, *44*, 1321−1326.

(11) Van Ruth, S. M.; Roozen, J. P.; Cozijnsen, J. L. Changes in flavour release from rehydrated diced bell peppers (*Capsicum annuum*) by artificial saliva components in three mouth model systems. *J. Sci. Food Agric.* **1995**, *67*, 189−196.

(12) Van Ruth, S. M.; Roozen, J. P. Influence of mastication and saliva on aroma release in a model mouth system. *Food Chem.* **2000**, *71*, 339−345.

(13) Van Ruth, S. M.; O'Connor, C. H.; Delahunty, C. M. Relationships between temporal release of aroma compounds in a model mouth system and their physico-chemical characteristics. *Food Chem.* **2000**, *71*, 393−399.

(14) Banavara, D. S.; Rabe, S.; Krings, U.; Berger, R. G. Modeling dynamic flavor release from water. *J. Agric. Food Chem.* **2002**, *50*, 6448−6452.

(15) De Roos, K. B.; Wolswinkel, K. Non-equilibrium partition model for predicting flavour release in the mouth. In *Trends in Flavour Research*; Maarse, H., van der Heij, D. G., Eds.; Elsevier Science: Amsterdam, The Netherlands, 1994; pp 15−32.

(16) Land, D. G. Perspectives on the effects of interactions on flavor perception: an overview. In *Flavor-food interactions*; McGorrin, R. J., Leland, J., Eds.; American Chemical Society: Washington, DC, 1996; pp 2−11.

(17) Taylor, A. J.; Linforth, R. S. T. Flavour release in the mouth. *Trends Food Sci. Technol.* **1996**, *7*, 444−448.

(18) Taylor, A. J.; Linforth, R. S. T.; Harvey, B. A.; Blake, A. Atmospheric pressure chemical ionisation mass spectrometry for in vivo analysis of volatile flavour release. *Food Chem.* **2000**, *71*, 327−338.

(19) Lindinger, W.; Hansel, A.; Jordan, A. On-line monitoring of volatile organic compounds at pptv levels by means of proton-transfer-reaction mass spectrometry (PTR-MS) - Medical applications, food control and environmental research. *Int. J. Mass Spectrom.* **1998**, *173*, 191−241.

(20) Linforth, R.; Taylor, A. J. Persistence of volatile compounds in the breath after their consumption in aqueous solutions. *J. Agric. Food Chem.* **2000**, *48*, 5419−23.

(21) Buettner, A.; Schieberle, P. Exhaled odorant measurement (EXOM) - a new approach to quantify the degree of in-mouth release of food aroma compounds. *Lebensm.-Wiss. Technol.* **2000**, *33*, 553−559.

(22) Buettner, A.; Beer, A.; Hannig, C.; Settles, M. Observation of the swallowing process by application of videofluoroscopy and real-time magnetic resonance imaging - consequences for retronasal aroma stimulation. *Chem. Senses* **2001**, *26*, 1211−1219.

(23) Weel, K. G. C.; Boelrijk, A. E. M.; Burger, J. J.; Gruppen, H.; Voragen, A. G. J.; Smit, G. A Protocol for Measurement of In Vivo Aroma Release from Beverages. *J. Food Sci.* **2003**, *68*, 1123−1128.

(24) Hogson, M.; Linforth, R. S. T.; Taylor, A. J. Simultaneous real-time measurements of mastication, swallowing, nasal airflow, and aroma release. *J. Agric. Food Chem.* **2003**, *51*, 5052−5057.

(25) Buettner, A.; Beer, A.; Hannig, C.; Settles, M.; Schieberle, P. Physiological and analytical studies on flavor perception dynamics as induced by the eating and swallowing process. *Food Qual. Pref.* **2002**, *13*, 497−504.

(26) Normand, V.; Avison, S.; Parker, A. Modeling the kinetics of flavour release during drinking. *Chem. Senses* **2004**, *29*, 235−245.

(27) Weel, K. G. C.; Boelrijk, A. E. M.; Burger, J. J.; Claassen, N. E.; Gruppen, H.; Voragen, A. G. J.; Smit, G. Effect of whey protein on the in vivo release of aldehydes. *J. Agric. Food Chem.* **2003**, *51*, 4746−4752.

(28) Murray, A. Concentration techniques for food, beverage industries. I. Evaporation. *Food Rev.* **1987**, *14*, 15.

(29) Keyhani, K.; Scherer, P. W.; Mozell, M. M. A numerical model of nasal odorant transport for the analysis of human olfaction. *J. Theor. Biol.* **1997**, *186*, 279−301.
(30) Deibler, K.; Acree, T. Effect of beverage base conditions on flavor release. In *Flavor Release*; Roberts, D. D., Taylor, A. J., Eds.; American Chemical Society: Washington, DC, 1999; pp 333−340.
(31) Friel, E. N.; Taylor, A. J. Effect of salivary components on volatile partitioning from solutions. *J. Agric. Food Chem.* **2001**, *49*, 3898−3905.
(32) Van Ruth, S. M.; Grossmann, I.; Geary, M.; Delahunty, C. M. Interactions between artificial saliva and 20 aroma compounds in water and oil model systems. *J. Agric. Food Chem.* **2001**, *49*, 2409−2413.
(33) Reid, R. C.; Prausnitz, J. M.; Poling, B. E. *Properties of gases and liquids*, 4th ed.; McGraw-Hill: New York, 1987.
(34) Cook, D. J.; Hollowood, T. A.; Linforth, R. S. T.; Taylor, A. J. Oral shear stress predicts flavour perception in viscous solutions. *Chem. Senses* **2003**, *28*, 11−23.
(35) Weel, K. G. C.; Boelrijk, A. E. M.; Burger, J. J.; Jacobs, M. A.; Gruppen, H.; Voragen, A. G. J.; Smit, G. Effect of emulsion properties on release of esters under static headspace, in vivo, and artificial throat conditions in relation to sensory intensity. *J. Agric. Food Chem.* **2004**, *52*, 6572−6577.

Received for review March 26, 2004. Revised manuscript received July 12, 2004. Accepted August 7, 2004. The work presented in this paper has been funded by Imperial Chemical Industries PLC (project SRF 2015).

JF049499X